A Real-Time Implementation of the Mobile WiMAX ARQ and Physical Layer

Pedro Suárez-Casal · Ángel Carro-Lagoa · José A. García-Naya · Paula Fraga-Lamas · Luis Castedo · Antonio Morales-Méndez

Abstract This paper presents an innovative software-defined radio architecture for the real-time implementation of WiMAX transceivers. The architecture consists of commercially available field-programmable gate array and digital signal processor modules. We show how the architecture can be used for the real-time implementation of a full-featured standard-compliant time-division duplex WiMAX physical layer together with the ARQ functionality of the MAC layer. Both the mobile and the base station contain a transmitter and a receiver to enable real-time concurrent downlink and uplink communications. The design supports the different configurations defined by the standard and the WiMAX Forum. This work also provides the verification and validation of the proposed real-time implementation based on repeatable and reproducible performance evaluation considering the reference scenarios defined by the WiMAX Forum, including both static and mobile scenarios. Typical figures of merit such as physical-layer bit and frame error rates and MAC-layer throughput are obtained with the help of a custom-made real-time channel emulator implementing the channel models defined by the WiMAX Forum.

Keywords IEEE 802.16e · WiMAX · Physical layer · SDR · FPGA · DSP · Downlink · Uplink · OFDMA · ARQ

P. Suárez-Casal · Á. Carro-Lagoa (✉) · J. A. García-Naya · P. Fraga-Lamas · L. Castedo

Department of Electronics and Systems, University of A Coruña, Facultade de Informática, Campus de Elviña, 15071 A Coruña, Spain
e-mail: acarro@udc.es

P. Suárez-Casal
e-mail: pedro.scasal@udc.es

J. A. García-Naya
e-mail: jagarcia@udc.es

P. Fraga-Lamas
e-mail: paula.fraga@udc.es

L. Castedo
e-mail: luis@udc.es

A. Morales-Méndez
Indra Sistemas, S.A., 28300 Aranjuez, Spain
e-mail: ammendez@indra.es

1 Introduction

Worldwide Interoperability for Microwave Access (WiMAX) was initially conceived for wireless broadband access, but evolved with time until becoming a candidate technology for the so-called 4G mobile networks. In late 90s, IEEE started the working group IEEE 802.16 to create a Point-to-Multi-Point (PMP) air interface alternative to cable and digital subscriber lines. The name WiMAX was coined by the WiMAX Forum, an organization constituted to promote the interoperability of the standard. The original standard was modified to produce the IEEE 802.16d standard for fixed applications. IEEE 802.16d uses Orthogonal Frequency-Division Multiplexing (OFDM) as the transmission scheme. In 2005, mobility support was incorporated based on Scalable Orthogonal Frequency-Division Multiple Access (SOFDMA), resulting in the amendment 802.16e, also known as Mobile WiMAX. Four years later, the standard IEEE 802.16-2009 was released to support both fixed and mobile wireless communications. A complete survey of the historical evolution of the standard up to 2010 can be found in [22]. Recently, in 2011, WiMAX evolved to 802.16m [2], which focuses on providing an advanced air interface to fulfill the requirements of IMT-Advanced while

maintaining backward compatibility with existing specifications. In August 2012, the IEEE 802.16-2012 [3] was released, consolidating material from IEEE 802.16j-2009 for relay-based networks and the amendment 802.16h-2010, which implements coexistence enhancement for license-exempt operation. Such a standard also incorporated the IEEE 802.16m-2011, but excluding the WirelessMAN Advanced Air Interface, which is now specified in the IEEE 802.16.1-2012 [5]. Finally, improvements focused on Machine-to-Machine (M2M) applications are examined in amendments 802.16p-2012 [4] and 802.16.1b-2012 [6].

The WiMAX physical layer is in charge of multiplexing user and system data together with control signaling in order to ensure a proper utilization of the radio resources. The WiMAX physical layer specifies how to map and how to allocate those resources as either reference signals or to form various physical channels. WiMAX supports several physical layer modes. Among them, OFDMA is the most appealing given its flexibility and ability to support multiple users at the same time.

WiMAX specifies both Frequency-Division Duplex (FDD) as well as Time-Division Duplex (TDD) operating modes. TDD was preferred in this work due to its capabilities for dealing with the asymmetrical uplink/downlink data flow. Despite these advantages, few works exist in the literature that address the complete and real-time implementation of OFDMA-TDD mobile communication physical layer. Existing works focus on performance analysis such as path-loss measurements using Fixed WiMAX commercial equipment in rural environments [14], tests in outdoor scenarios employing commercial Mobile WiMAX equipment [30], or evaluations of the IEEE 802.16e OFDMA downlink in vehicular environments (ITU-R M.1225) [10]. In this context, references considering simulations [20], non-real-time deployments [13, 19], and Fixed WiMAX implementations [16] were found. However, none of the aforementioned approaches accounts for software constraints or hardware limitations.

The experimental validation of prototype baseband systems employing real-time hardware demonstrators confronts several challenges such as enormous design complexity, long development time, high costs and manpower, or dealing with unsurmountable hardware issues. To the authors knowledge, although several papers can be found in the literature describing real-time implementation and validation of downlink [15] or uplink channels [29], no work has been found dealing with both at the same time. It is worth mentioning that Mobile WiMAX duplex communications in a system-on-chip platform can be found in [9].

Studies that incorporate MAC layer functionalities provide a more realistic evaluation of the actual performance of a wireless communication system, especially when measuring meaningful metrics such as throughput. A detailed description of the WiMAX ARQ mechanism and a performance analysis using a simulated environment can be found in [24]. Theoretical analysis of the throughput achievable at MAC level taking into account some features of the WiMAX physical layer can be found in [23]. Some works devoted to study the effect of particular parameters of the WiMAX ARQ or H-ARQ mechanisms in order to improve specific metrics are [7, 12, 17]. These references usually rely on simulations of the physical layer using simplified channel models, thus the behavior of the systems cannot be reliably outlined under more realistic conditions. Implementations of full-featured MAC layers using network processors with a detailed design description and resource utilization can also be found [28].

This paper details a real-time implementation and validation of full-duplex OFDMA-TDD WiMAX transceivers that contain a complete physical layer. A reduced version of the MAC layer with only basic features such as ARQ is also included, which allows for more meaningful evaluation of the performance of WiMAX transceivers. Additionally, the paper also includes a very rich performance evaluation of the real-time implementations of both physical and MAC layers based on representative figures of merit such as bit and frame error rates or throughput and considering the reference scenarios defined by the WiMAX Forum, including both static and mobile scenarios. A description of an implementation of the physical layer can be found in a previous work [8] as well as results for synchronization and other physical-level metrics. The present work extends that architecture and shows new results which can be obtained with the new implemented features.

The remainder of this article is organized as follows. Sections 2 and 3 provide a brief description of the Mobile WiMAX physical and MAC layers, followed by the definition of the proposed hardware architecture in Section 4. Section 5 details the hardware components and the mapping of the real-time tasks to the hardware resources. The amount of resources consumed by the implementation is also detailed. Section 6 addresses the validation of the implementation, which is carried out by means of performance evaluations over ITU-R channel models generated by a custom-made channel emulator. Finally, Section 7 is devoted to the conclusions.

2 Mobile WiMAX Physical Layer

Mobile WiMAX is based on the OFDMA physical layer defined in the IEEE 802.16e standard. It supports both TDD and FDD operation modes while allowing for variable bandwidth and a scalable number of subcarriers ranging from

128 to 2048. Furthermore, the WiMAX Forum specifies five profiles for interoperability as shown in Table 1. Such profiles combine different FFT sizes, bandwidths, and sampling frequencies.

Figure 1 plots the block diagram of the physical layer of a WiMAX transmitter as defined in the IEEE 802.16e standard. In TDD, each frame is divided into downlink and uplink subframes. The downlink subframe consists of a preamble followed by a Frame Control Header (FCH), and DL-MAP and UL-MAP messages. If an UL-MAP message is sent to describe the uplink structure, it must be included in the first burst defined in the DL-MAP.

The mapping of bursts on subframes can be done using different permutation schemes such as non-adjacent groupings with Partial Usage of Subcarriers (PUSC) or Full Usage of Subcarriers (FUSC). The smallest data allocation unit is the slot, which is used to specify the time-frequency regions for data in the bursts. The slot definition varies according to the subcarrier grouping scheme. Uplink resources are shared among Mobile Stations (MSs) and their management is centralized at the Base Station (BS), which decides the amount of slots to be assigned to each MS based on the Quality-of-Service (QoS) parameters and bandwidth requirements for each connection. Additionally, the so-called ranging regions can be defined in the uplink to allow subscriber stations to perform network entry or to improve uplink synchronization parameters.

Data and pilot subcarriers are scrambled before the Inverse Fast Fourier Transform (IFFT) and the Cyclic Prefix (CP) insertion are applied (see Fig. 1). Notice that the length of the cyclic prefix can take one of the following values: 1/4, 1/8, 1/16, and 1/32.

In the IEEE 802.16e-2005, the channel coding stage consists of the following steps: data randomization, channel coding, bit-interleaving, repetition coding, and symbol mapping. Data randomization is performed in both the uplink and the downlink employing the output of a maximum-length shift-register sequence initialized at the beginning of every FEC block. Such a FEC block consists of an integer number of subchannels. Channel coding is performed on a per-FEC-block basis employing one of the schemes defined in the standard, namely, Tail-Biting Convolutional Codes (TBCC), Block Turbo Codes (BTC), Convolutional Turbo Codes (CTC), or Low-Density Parity Check Codes (LDPC). Additionally, variable coding rate and modulation are supported, thus enabling for Adaptive Modulation and Coding (AMC) capabilities. Furthermore, Repetition coding with factors of 2, 4, or 6 are employed to increase the resilience of important control data. Finally, the coded bits are mapped into QPSK, 16-QAM, or 64-QAM constellations at the modulation stage.

Table 1 Mobile WiMAX profiles.

WiMAX profile	Channel bandwidth	Sampling frequency	FFT size
# 1	3.5 MHz	4 MHz	512
# 2	5 MHz	5.6 MHz	512
# 3	7 MHz	8 MHz	1024
# 4	8.75 MHz	10 MHz	1024
# 5	10 MHz	11.2 MHz	1024

3 Mobile WiMAX MAC Layer

The MAC layer provides an interface between the higher-level transport layers and the physical layer. The packets received from the higher-level layers, called MAC Service Data Units (MSDUs), are reorganized into MAC Protocol Data Units (MPDUs) and sent to the PHY layer. The reverse operation is done at the receiver side.

The MAC layer is divided into three sublayers: the Convergence Sublayer (CS), the Common Part Sublayer (CPS), and the security sublayer. The CS maps the external network data into MSDUs allowing the MAC layer to be used with several protocols, like IP or Ethernet. Therefore, the CS has a set of classification rules which are used to assign the appropriate service flow to the higher-level layer packets. The CS can perform other tasks to reduce the overheads of the higher-level layers like Packet Header Suppression (PHS) or RObust Header Compression (ROHC). The CPS is the core subsystem of the WiMAX MAC, providing all the needed mechanisms for connection establishment and maintenance, bandwidth allocation, Quality of Service (QoS) provisioning, etc. The security sublayer is embedded inside the CPS to provide authentication, secure key exchange and encryption functionalities.

3.1 MPDU Generation

The WiMAX MAC layer is connection-oriented. Hence, MSDUs arriving from higher-level layers must be classified on MAC connections before transmission. These connections have associated the relevant parameters to packet transmission, such as the QoS requirements and the encryption keys. All information carried into MPDUs is always linked to a unique connection, but a wide range of possibilities regarding its generation is supported. Fragments of different MSDUs can be packed into a MPDU, and a MSDU can be split into several MPDUs. Also, if a group of MPDUs is going to be transmitted under the same physical modulation and coding, they can be concatenated into the same physical burst, even if they come from different MAC connections.

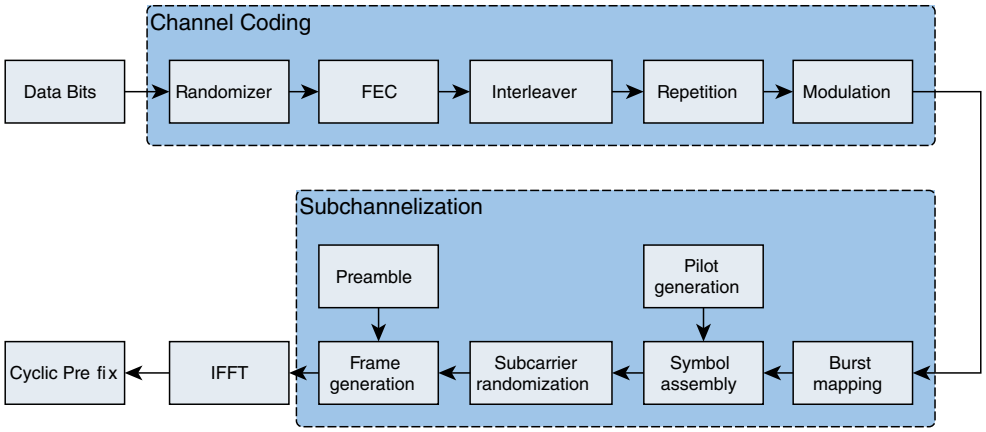

Figure 1 IEEE 802.16 transmitter block diagram.

Besides routing traffic from higher-level layers, MPDUs can also carry management messages of the MAC layer. These messages are meant to control processes which are exclusive of this layer, such as conveying information about the structure of the downlink and uplink subframes, managing network entry and initialization of new MSs, or completing secure authentication and key exchanges. In this case dedicated MAC connections are used, while packing and fragmentation of messages is not allowed.

Regarding their structure, all MPDUs are preceded by a six-byte-header, and then a set of optional fields can appear depending on the configuration of the connection as well as the payload with the information to be transmitted. There is a special type of MPDU with only a header and no payload, used exclusively in the uplink, whose purpose is to signal control information to the BS in a very compact form.

3.2 ARQ Mechanism

The Automatic Repeat Request (ARQ) mechanism allows for the retransmission of erroneous decoded MPDUs and works at MAC connection level. To provide this functionality, the MSDUs are divided in fixed-length blocks and numbered by assigning a Block Sequence Number (BSN) to each block. The transmitter and receiver sides use a fixed-size window to manage the block states. The receiver side sends ARQ feedback messages to inform the state of its window, so the transmitter knows which blocks need to be retransmitted. The ARQ mechanism is managed by the transmitter and receiver state machines using timers to control the state changes of each block.

The ARQ performance is influenced by several parameters such as block size, window size and maximum waiting interval of the timers. These parameters are established on connection creation, and they are stored in the service flow associated to the connection. The ARQ feedback intensity is not specified in the standard and it is left to the designer's choice.

4 Proposed System Architecture

The real-time implementation described in this section focuses on the mandatory parts of the Mobile WiMAX physical layer for base and subscriber stations. It employs the OFDMA-TDD frame structure, the PUSC permutation scheme both in the downlink and the uplink subframes, the ranging, and the channel coding based on TBCC.

4.1 Downlink Synchronization

Downlink synchronization consists of frame and symbol detection at the MS. Such tasks take advantage of the correlation properties exhibited by the preamble defined in the standard as well as those found in OFDM symbols when the cyclic prefix is included. The subsystem in charge of the downlink synchronization is shown in Fig. 2.

Preambles in Mobile WiMAX have a fixed structure with two guard subcarriers inserted between each pilot subcarrier. Their values are selected from a predefined set depending on the segment and base-station cell identifier. Frame detection is based on the Repetition Property Based (RPB) autocorrelation metric [25]. Next, two frequency offset estimations are obtained computing the angle of the previously declared autocorrelation values. The first one is extracted directly from the preamble, allowing for a wide frequency offset acquisition range. The second one is gathered from the cyclic prefixes, hence tracking the frequency offset on a per-OFDM-symbol basis.

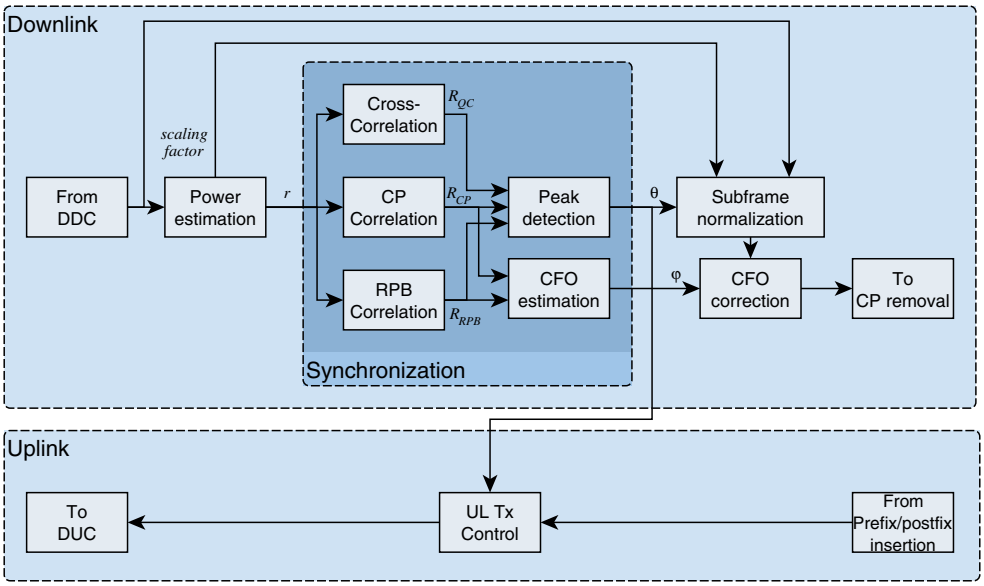

Figure 2 Downlink synchronization subsystem.

4.2 Uplink Synchronization

Physical layers based on OFDMA require that uplink frames arrive at the BS at the same time and with a significant accuracy. This can only be achieved if all users are synchronized with the BS before the communication takes place. WiMAX standard states that the Round-Trip Delay (RTD) between the MS and the BS must be known beforehand by the MS. This is possible thanks to the so-called ranging step.

For that purpose, MSs generate Pseudo Noise (PN) sequences from a shift register that are transmitted in specific regions of the uplink subframe. Such regions have to be reserved by the BS in a contention-based policy. At the receiver side (in the uplink), the BS detects the arrival of a ranging code and then it estimates the synchronization parameters. Finally, the MS adjusts its synchronization parameters from the base-station estimates sent back to the MS in a Medium Access Control (MAC) management message.

The standard defines different operation types depending on the current connection state: initial ranging on network entry, periodic ranging to update variations, bandwidth requests, and handover. During the initial ranging, OFDM symbols containing ranging codes are transmitted by the MS in pairs, the first one with a cyclic prefix, while the second one also adds a cyclic postfix, hence allowing for a wider time-synchronization margin.

Code detection and time-offset estimation at the BS takes place at the frequency domain over each received OFDM symbol. First, a power threshold (see Fig. 2) followed by cross-correlation between the arriving subcarriers and all possible ranging codes is performed [18]. Once the ranging code is known, the received PN sequence is mapped back to the OFDM symbol. Since the initial ranging forces MSs to transmit the same ranging code twice in two consecutive symbols, this property is exploited to extract the frequency offset through a correlation.

4.3 Subchannelization and Channel Equalization

Subchannelization involves interleaving and randomizing subcarriers followed by a permutation scheme and a pilot pattern. The BS specifies this structure for each frame using the dedicated DL-MAP and UL-MAP messages. Therefore, DL-MAP messages become critical since most of the processing of the downlink subframe at the receiver cannot start until this message has been completely decoded. On the other hand, subcarrier randomization in the uplink cannot be applied to the ranging bursts. Hence this process depends entirely on the uplink burst scheme defined by the BS. We assign this task to the Digital Signal Processor (DSP) to provide the maximum flexibility with respect to the different FFT sizes, burst mapping, and eventual support of other permutation schemes (see Fig. 3).

Channel estimation and equalization is performed by inverting the pilot subcarriers and linearly interpolating the computed values for the remainder subcarriers.

4.4 Channel Coding

The proposed design supports a variable-rate TBCC coding scheme with constellation sizes varying from QPSK to 64-QAM, both in the downlink and the uplink.

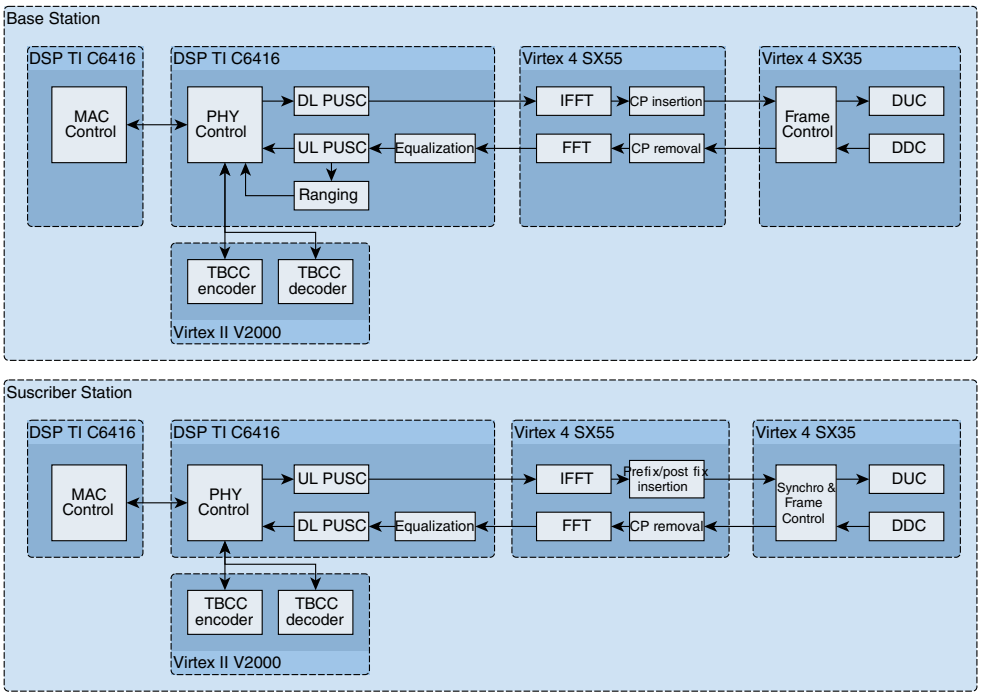

Figure 3 Hardware components and real-time software tasks with their allocation for the BS and the MS.

There are several techniques to design TBCC using standard convolutional encoders and Viterbi decoders [11]. The chosen technique offers a good trade-off between computational complexity and performance. The encoder is implemented adding a cyclic prefix to each FEC block with a size equal to the constraint length (in the case of WiMAX, such a value is set to 7). On the other hand, the decoder concatenates the first bits of the block at the end, and vice versa, hence removing the additional bits from the decoder output.

The size of the chunks added at the beginning and at the end of the blocks is equal to the traceback length of the Viterbi decoder. If a block is shorter than the traceback length, it is just sent three times to the decoder and only the output corresponding to the second repetition is considered.

Additionally, the decoder computes a Carrier-to-Interference Noise Ratio (CINR) metric employing a soft-demapper to estimate the transmitted symbols. It was verified that the algorithm provides accurate values of the CINR as long as decision errors are low. Otherwise, the CINR is overestimated.

Channel coding is mainly implemented in a Virtex II FPGA (see Fig. 3), although the optional repetition coding step performed over the constellation-mapped data and the processing control are both carried out in the DSP, using the FPGA as a coprocessor.

4.5 Physical Layer Control

Separation between MAC-level and physical-layer-level processing is obtained using the so-called OFDMA physical-layer Service Access Point (SAP) specification defined by Intel for its BSs [1]. Such a SAP provides the description of the subframes, it sends and acquires data bursts, and it transmits and detects ranging codes.

The subframe structure is transferred to the MS through MAC management messages (DL-MAP, UL-MAP, Downlink Channel Descriptor (DCD), and Uplink Channel Descriptor (UCD)). Mobile WiMAX requires data bursts to be rectangular-shaped while spanning a multiple of two symbols in time and a multiple of a subchannel in frequency (the so-called slot unit). Although the standard allows for more than a single burst per MS, the corresponding DL-MAP overhead is increased. Moreover, the standard also allows for more than a single connection packed into a burst. Finally, the BS has to distribute the available resources between users, while guaranteeing their QoS requirements.

4.6 MAC Layer Control

This task is the main responsible of the operations done inside the MAC Layer. Our implementation provides basic MAC functionalities to allow for transmission of data flows with ARQ in order to make meaningful performance measurements with the implemented PHY layer. Figure 4 shows the behaviour of the BS transmitting Service Data Units (SDUs) arriving from other layers. First of all, the SDUs are queued and the Service Data Units (SDUs) transmission module takes fragments of the next SDU to map into PDUs. This process is done with the help of a frame management module responsible for the accounting of the

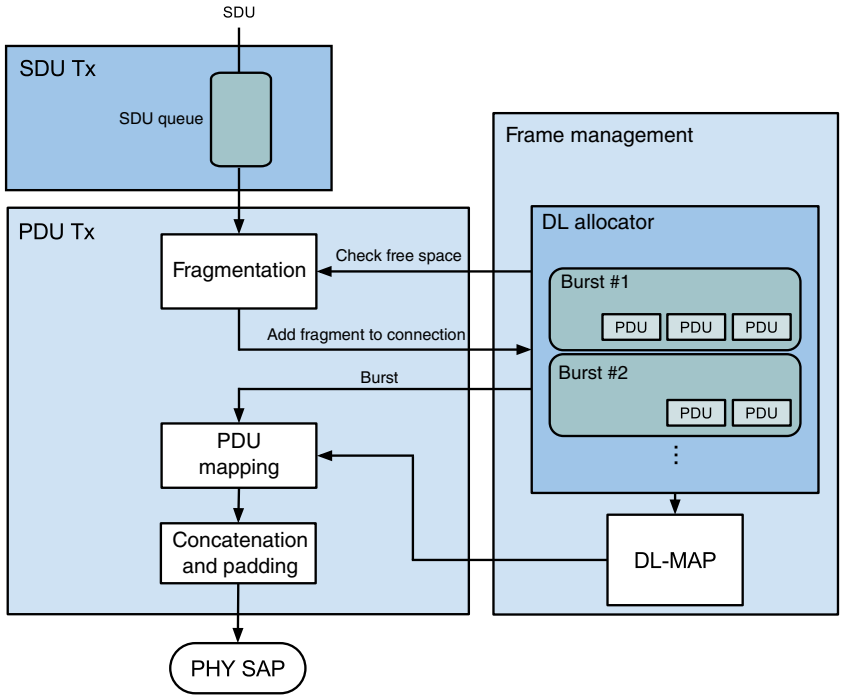

Figure 4 Diagram of the burst management in the BS.

radio resources available given the current profile configuration. The available space inside the downlink subframe is checked iteratively, and while it is possible, new fragments are taken from the SDU queue and added to the PDUs. Finally, bursts with their corresponding PDUs are mapped into buffers and sent to the PHY layer with the help of its SAP. As a result of this process, a DL-MAP management message is also generated with the description of the bursts. This message is inserted into a PDU, mapped to a burst, and sent to the PHY layer like a regular burst.

Multiple burst-mapping proposals for Mobile WiMAX are presented in [26]. Our implementation uses the so-called Ohseki algorithm [21], a reference algorithm considering complexity, requested bandwidth, and the shape of the downlink burst. The frame management module implements this algorithm and uses information about the burst profile used by the target MS to decide the burst to be used to map its PDUs. Potentially, all users sharing the same burst profile (i.e. modulation and channel coding) would receive all their PDUs inside the same burst.

Resource management in the uplink is more flexible since it is only necessary to indicate the number of slots allocated to each station. The size of such allocations should be decided by the MAC layer considering the QoS constraints and the bandwidth requests received from each user. The current implementation equally distributes all the available bandwidth between the users. The MS manages the available space using a similar scheme in the downlink, but using only one burst with the size assigned in the UL-MAP management message by the BS, hence simplifying the allocation process.

When the ARQ is enabled, the fragmentation process in Fig. 4 is done following the rules of the ARQ process. In this case the feedback information from the MS is used to know whether a new or an old fragment must be sent. The frame management module also takes this into account, and when new SDU fragments are added to PDUs, subheaders with the sequence numbers are appended.

5 Hardware Description

In the proposed design for a bi-directional TDD WiMAX transceiver, MS and BS were implemented utilizing the same type of hardware elements based on Commercial Off-The-Shelf (COTS) components. An overview of the architecture defined for the BS and the MS is shown in Fig. 3. Each station consists of four different FPGAs and a DSP module placed on a Peripheral Component Interconnect (PCI) carrier board.

The first module contains a Texas Instruments TMS320C6416 DSP. The second module contains a Texas Instruments TMS320C6416 DSP together with a Xilinx Virtex-II XC2V2000 FPGA. The third module has a Xilinx Virtex-4 XC4VSX55 FPGA, while the fourth one is equipped with a Virtex-4 XC4VSX35 FPGA together with an analog add-on module containing a dual

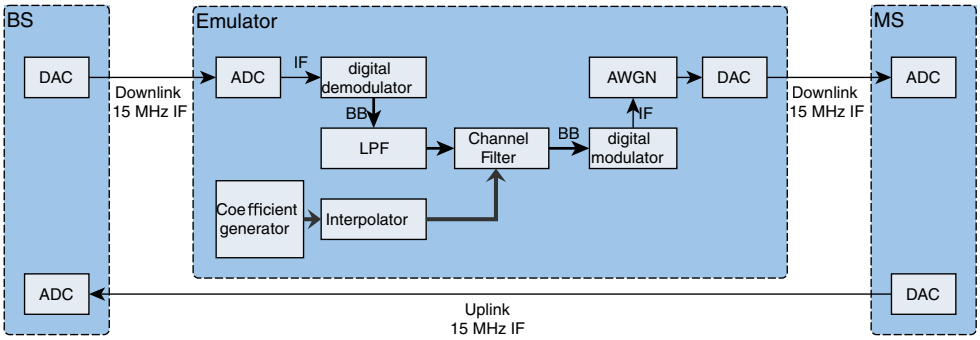

Figure 5 Real-time custom-made channel emulator utilized for validating the implementation.

Digital-to-Analog Converter (DAC) and a pair of Analog-to-Digital Converters (ADCs). Note that both Virtex-4 FPGAs are equipped with a large number of embedded multipliers, hence enabling intensive signal processing operations.

Data exchange between hardware modules is achieved using proprietary buses that can reach up to 400 MB/s, together with control-data buses limited to 20 MB/s. A PCI bus links the carrier board containing the hardware modules to a host computer.

In order to validate the real-time implementation as well as to assess the performance of the system, a channel emulator was implemented on a Xilinx Xtreme DSP Development Kit consisting of a Virtex-4 FPGA plus a couple of DACs and ADCs (see Fig. 5).

5.1 Digital Up/Down Conversion

Digital Up-Conversion (DUC) and Digital Down-Conversion (DDC) adapt the signals to the sampling rate of ADCs and DACs (see Fig. 3). In the case of the DUC, the following tasks are done: upsampling, pulse shaping, and I/Q modulation to a configurable intermediate frequency. The DDC performs the complementary operations in the reverse order. The chosen profiles selected by the WiMAX Forum are supported by means of five different bit-streams for the FPGAs. Each bit-stream has a different up/down-sampling factor. Since the DACs and the ADCs are configured with a sampling frequency of 80 MHz, the factors for each profile are 20, 100/7, 10, 8, and 50/7 for profiles 1 to 5, respectively (see Table 1). Each FPGA bit-stream also has a different optimized combination of interpolation/decimation filters in order to efficiently implement these sampling-rate conversions [27].

5.2 Resource Utilization

FPGA designs were implemented using the Xilinx System Generator and built with the Xilinx ISE 10.1. The resource utilization of the FPGAs is shown considering Slices, LUTs, RAMB16s, and multipliers for both BS and MS in Table 2.

The relatively high consumption of FPGA resources is explained because all FPGA tasks were implemented using the System Generator high-level development tool. Therefore, the implementation process becomes easier and faster,

Table 2 FPGA resource utilization.

Base station	Virtex-II V2000	Virtex-4 SX55	Virtex-4 SX35
Slices	10131/10752 (94 %)	13785/24576 (56 %)	6580/15360 (41 %)
LUTs	13509/21504 (62 %)	18356/49152 (37 %)	8261/30720 (26 %)
RAMB16s	52/56 (92 %)	113/320 (35 %)	45/192 (23 %)
Multipliers	2/56 (3 %)	116/512 (22 %)	24/192 (12 %)
Mobile station	**Virtex-II V2000**	**Virtex-4 SX55**	**Virtex-4 SX35**
Slices	10131/10752 (94 %)	14692/24576 (59 %)	15358/15360 (99 %)
LUTs	13509/21504 (62 %)	19951/49152 (40 %)	22625/30720 (73 %)
RAMB16s	52/56 (92 %)	114/320 (35 %)	52/192 (27 %)
Multipliers	2/56 (3 %)	117/512 (22 %)	70/192 (36 %)

Table 3 ITU-R M.1225 channel models.

	Pedestrian A	Pedestrian B	Vehicular A
Number of paths	4	6	6
Power of each path [dB]	0, −9.7, −19.2, −22.8	0, −0.9, −4.9, −8.0, −7.8, −23.9	0, −1.0, −9.0, −10.0, −15.0, −20.0
Path delay [ns]	0, 110, 190, 410	0, 200, 800, 1200, 2300, 3700	0, 310, 710, 1090, 1730, 2510
Speed [km/h]	3	3	60, 120

but the price to be paid is a non-optimum code in terms of resource utilization. On the other hand, the higher resource utilization at the MS is first due to the synchronization block, which requires 68 % of the slices available at the Virtex-4 SX35, and second due to the concatenation of cyclic postfixes at the IFFT output. The utilization of a large FPGA such as the Virtex-4 SX55 allows for a pipelined architecture dedicated to the FFT implementation. In case of the Virtex-II, an optimized FEC design was required due to the limited resources available.

Finally, apart from subchannelization, channel estimation and equalization, subcarrier mapping, and ranging (only at the BS); the SAP protocol, the minimum functionalities from the MAC required for the bi-directional operation, and data exchange with the host are all carried out by the DSP, thus demanding a significant amount of resources from the DSP.

6 Performance Evaluation

This section describes the performance evaluation of the developed bi-directional TDD WiMAX transceiver. A diagram of the setup utilized is shown in Fig. 5. For evaluating the downlink in a repeatable and reproducible fashion, the corresponding downlink subframes are transmitted across the channel emulator, while the uplink is connected with a cable. The reverse configuration is considered for evaluating the uplink. This setup is used to obtain the BER measurements. In the throughput measurements, downlink and uplink subframes are transmitted across the channel emulator using power splitters to share the channel emulator in both directions.

The custom-made, real-time channel emulator was configured following the WiMAX Forum recommendations. Therefore, ITU-R M.1225 Pedestrian A at 3 km/h,

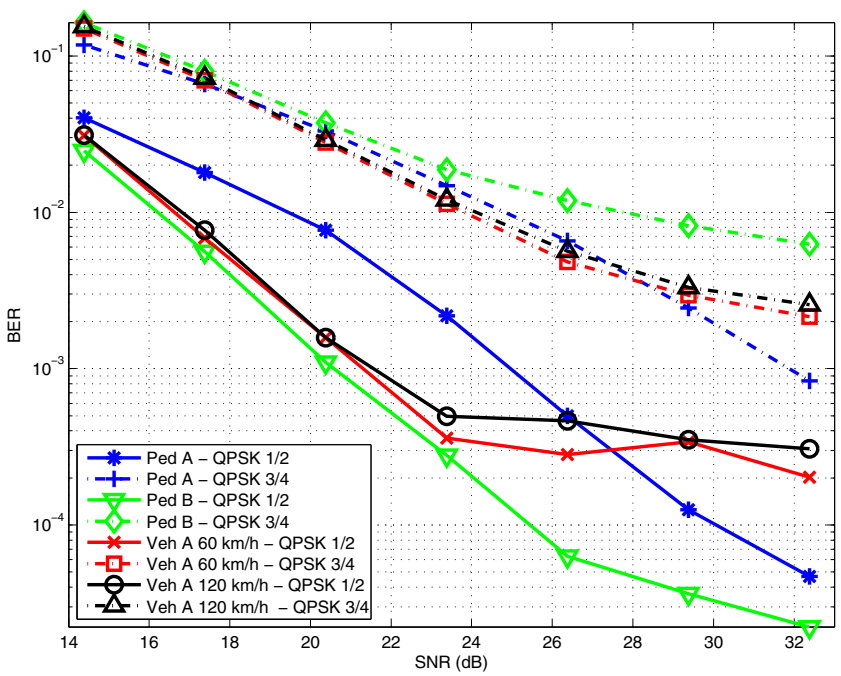

Figure 6 Coded BER in the downlink.

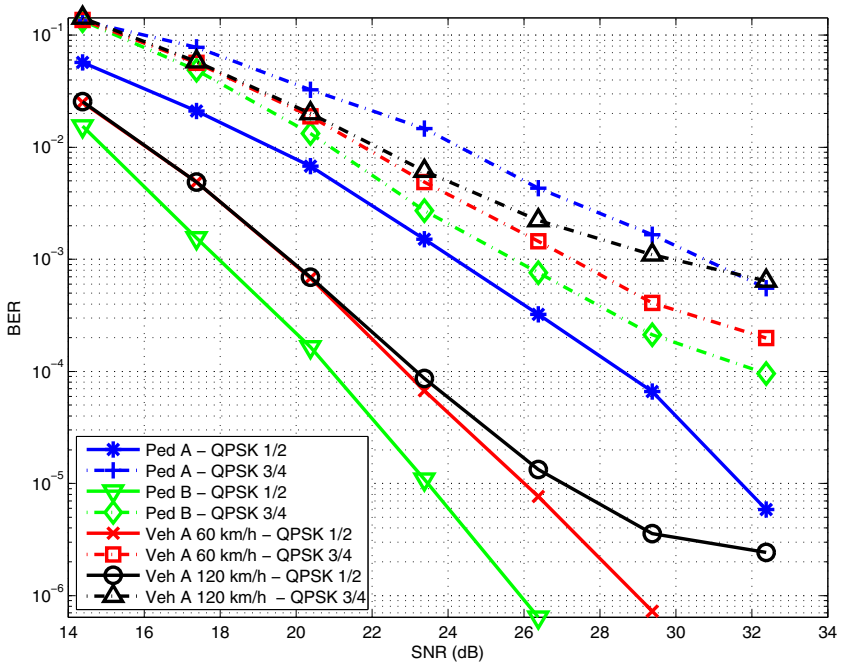

Figure 7 Coded BER in the uplink.

Pedestrian B at 3 km/h, Vehicular A at 60 and at 120 km/h were considered assuming the tapped-delay-line characteristics summarized in Table 3. Notice that frequency selectivity exhibited by Pedestrian A is very low, whereas Pedestrian B and Vehicular A models provide richer multipath diversity and higher path delay spread than Pedestrian A.

Doppler spread emulation uses the Jakes Doppler power spectrum density assuming transmissions at 2.4 GHz. Note also that the maximum channel delay (3.7 μs) does not exceed in any case the default 1/8 cyclic prefix length (11.4 μs). Consequently, the system is immune to Inter-Symbol Interference (ISI).

In order to obtain adequate performance metrics with respect to the SNR, the AWGN generator included in the channel emulator is calibrated to match the SNR estimation obtained during the synchronization process.

BER measurements are carried out considering a known structure for the subframes in order to avoid the case in

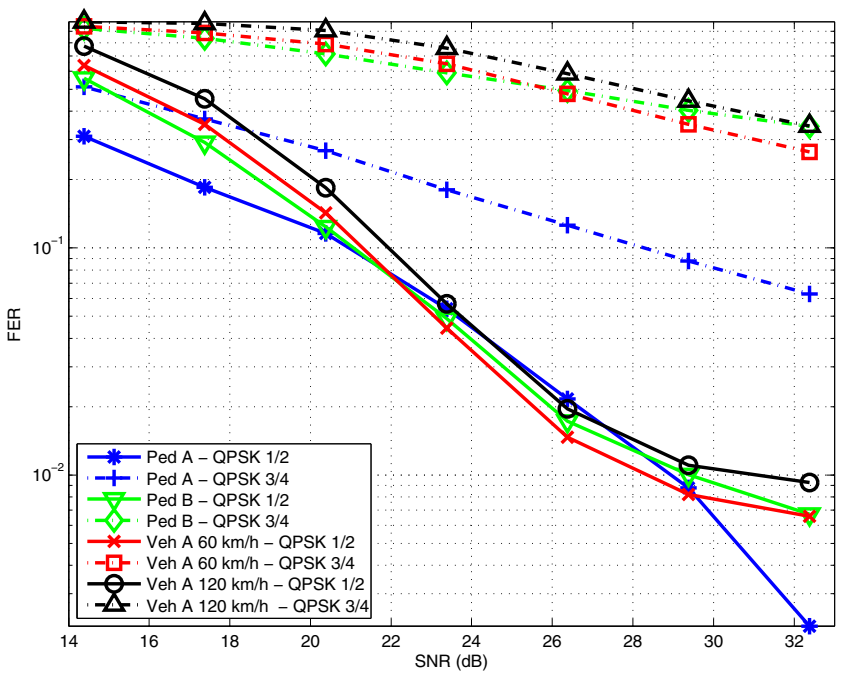

Figure 8 FER in the downlink. Bursts of 6480 bits for QPSK 1/2 and 9720 bits for QPSK 3/4.

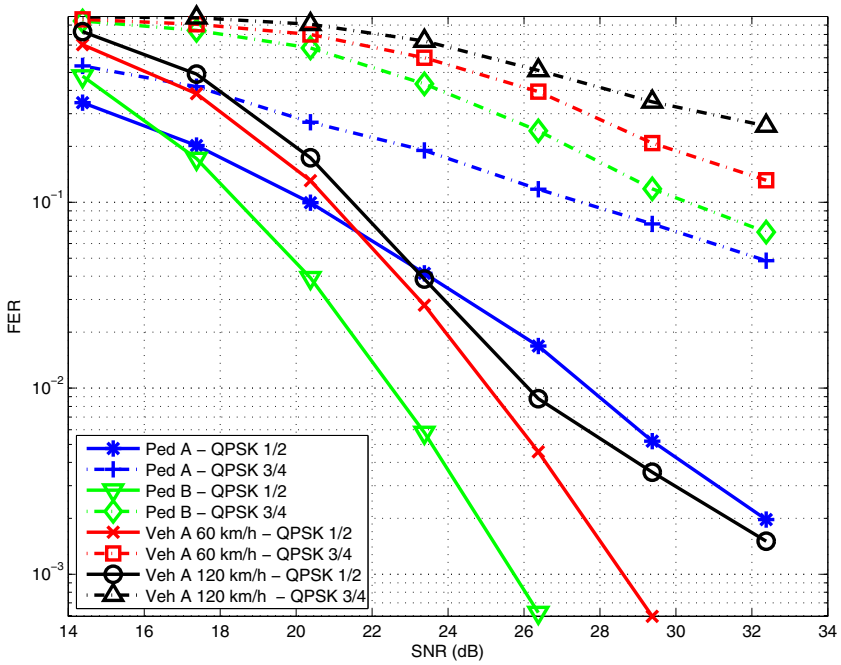

Figure 9 FER in the uplink. Bursts of 10080 bits for QPSK 1/2 and 15120 bits for QPSK 3/4.

Table 4 Throughput measurement configuration.

Parameter	Value
PHY	OFDMA
WiMAX Profile	8.75-MHz
Duplexing mode	TDD
Cyclic prefix length	1/8
DL/UL symbols	25/18
Frame duration	5 ms
Permutation schemes	DL/UL PUSC
DL/UL-MAP MCS	QPSK 1/2
Fragmentation	ON
Packing	ON
CRC	ON
PDU size	max. 2047 bytes
ARQ	ON
ARQ feedback types	all
ARQ_WINDOW_SIZE	1024 blocks
ARQ_BLOCK_SIZE	32 bytes
ARQ_RETRY_TIMEOUT	20 ms
ARQ_BLOCK_LIFETIME	50 s
ARQ_RX_PURGE_TIMEOUT	50 s
ARQ_SYNC_LOSS_TIMEOUT	OFF
ARQ_DELIVER_IN_ORDER	ON
SNRs	14, 17,..., 32
Transmission time per SNR	200 s
SDU size	1024 bytes
QPSK 1/2 max. throughput	2016 kbit/s
QPSK 3/4 max. throughput	3024 kbit/s

which FCH or the DL-MAP messages cannot be decoded correctly. The modulation and coding used in the following figures are QPSK and TBCC with 1/2 and 3/4 code rates. Figure 6 presents the BER for the 8.75-MHz downlink profile when the ITU-R channel models are employed.

BER measurements for the uplink transmission corresponding to the 8.75-MHz profile are shown in Fig. 7. An improvement with respect to the downlink transmission is observed. Although surprising in principle, this behaviour is perfectly justified when comparing the pilot structure of the uplink and downlink subframes. The effect is especially outstanding in the case of the Pedestrian B channel model. Due to the limited coherence time of Vehicular A channel models, there is a channel estimation error causing the error floor observed in Figs. 6 and 7. Also, a large loss is observed when comparing the same channel with different coding rates, being the differences more accute in Pedestrian B channel scenario. This is due to the higher frequency selectivity (i.e. multipath diversity) exhibited by this channel model. Such frequency selectivity is significantly better exploited by the system setup with code rate 1/2. Note that code rate does not impact performance so significantly when considering channel models with low frequency selectivity such as Pedestrian A.

Figures 8 and 9 show the Frame Error Rate (FER) when transmitting over the ITU-R channel models for the downlink and the uplink, respectively. The measured burst in the downlink occupies 15 subchannels along 18 OFDM symbols. This corresponds to a total of 6480 data subcarriers per downlink subframe. In the uplink measurement, the burst

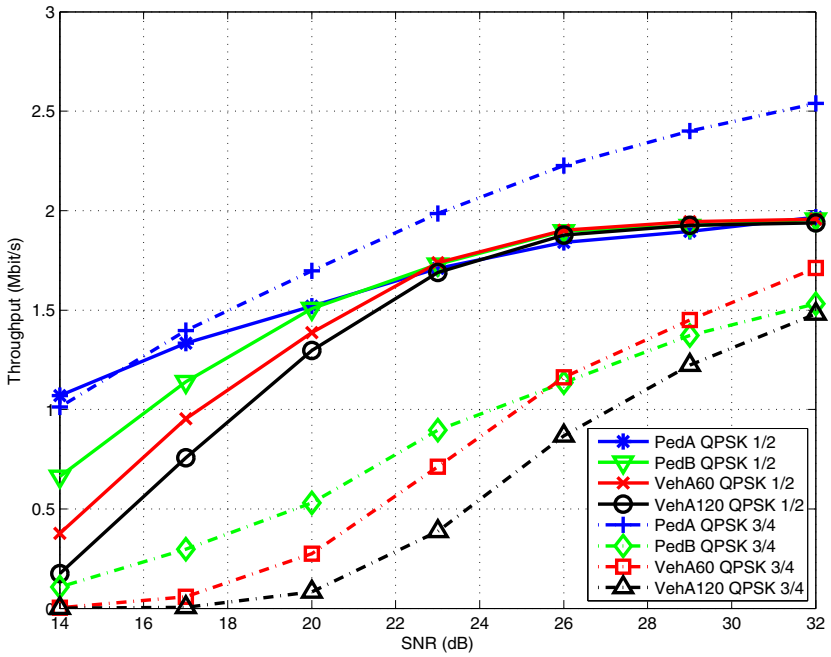

Figure 10 Throughput in the downlink.

occupies the complete subframe with 10 080 data subcarriers per uplink subframe. The downlink FER results are consistent with the downlink Bit Error Rate (BER) ones. The only significant difference is the worse results in the Pedestrian B caused by the higher frequency selectivity, which increases the probability of isolated errors in every burst. This results in higher FER but does not affect significantly the BER measurement. The uplink FER results are also consistent with the measurement of the BER in the uplink. In general, the results of Pedestrian A are improved when the FER is measured since the erroneous frames occur less often, but in those cases large error rates are obtained due to the lower multipath diversity.

Throughput measurements were performed over the same ITU-R channels, in this case affecting both downlink and uplink subframes at the same time in order that the ARQ feedback messages can also be corrupted. The channel emulator is shared in both directions in order to simulate

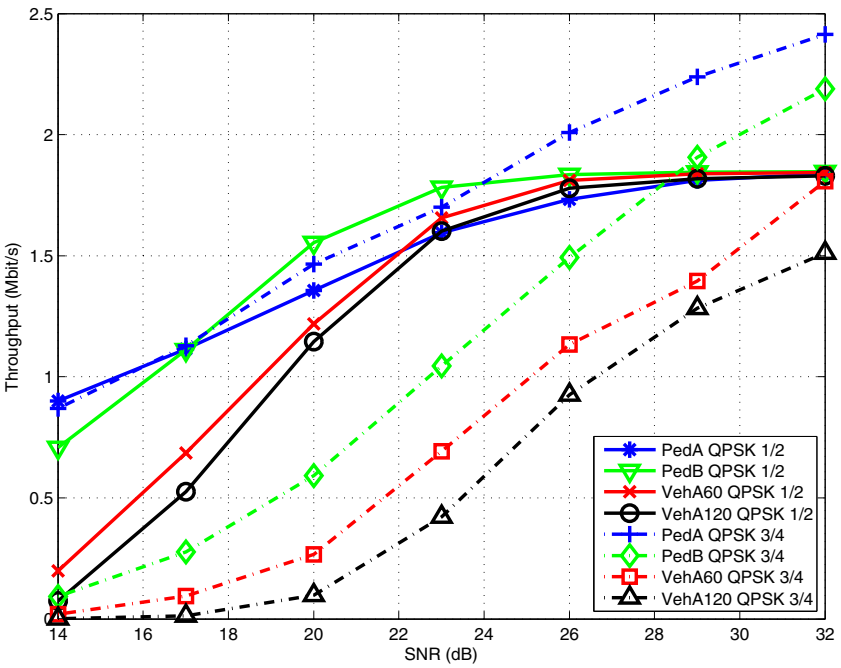

Figure 11 Throughput in the uplink.

the channel reciprocity characteristic of TDD systems. For each measurement, 40 000 frames were transmitted, i.e. the transmissions lasted 200 s.

The complete configuration parameters of the experiments are shown in Table 4. During each measurement, SDUs of 1024 bytes are continuously added to the transmit queue. The generated PDUs are filled with the 32 bytes ARQ blocks up to the maximum allowed size of 2047 bytes. This minimizes the overhead introduced by the PDU header but increases the error probability.

Figures 10 and 11 show the throughput values obtained with this configuration for both the downlink and the uplink. It can be seen that the QPSK 1/2 configuration almost achieves the maximum raw throughput of 2016 kbit/s. There is some overhead added by the generation of PDUs and the unused burst space, which cannot always be completely filled, and some padding has to be added. In the uplink, the periodical addition of reserved ranging bursts also reduces the maximum achievable throughput. In the downlink (DL), QPSK 3/4 configuration outperforms the QPSK 1/2 throughput at high SNRs for the Pedestrian A channel, while in the uplink (UL), the Pedestrian B and the Vehicular A at 60 km/h channels exhibit better results in QPSK 3/4 at high SNRs. Nevertheless, it is not possible to achieve the maximum throughput in the SNR levels tested in these scenarios because the maximum measured throughput was 2.5 Mbit/s. Finally, all the throughput values obtained are consistent with the FER measurements shown in Figs. 8 and 9.

7 Conclusion

In this paper we have proposed the design, implementation and validation of two real-time WiMAX transceivers, one for the BS and another for the MS. Transceivers implement a full featured bi-directional TDD physical layer and the ARQ functionalities of the MAC layer, all of them compliant with the WiMAX standard. We have described the utilized SDR hardware architecture consisting of commercial off-the-shelf modules based on FPGAs and DSPs. We have explained in detail most of the design decisions with the aim of obtaining an efficient utilization of the FPGA resources.

The implementation is validated in a repeatable and reproducible way by means of performance measurements carried out with the help of a real-time, custom-made channel emulator. Such channel emulator implements AWGN as well as the Pedestrian A and B, and Vehicular A channel models recommended by the WiMAX Forum.

Firstly, BER measurements were carried out for both the uplink and the downlink for the 8.75-MHz profile. Secondly, FER measurements are also provided for both the downlink and the uplink. Finally, throughput measurements including the MAC layer as well as the ARQ mechanism are also provided with the aim of assessing the actual performance of the complete WiMAX system in realistic propagation conditions. The measurement results confirm that the proposed implementation is suitable for the scenarios modeled with the aforementioned channel models.

Acknowledgments This work has been partially supported by Indra Sistemas S.A. and the Spanish Ministry of Defence with the technical direction of PEC/ITM under grant DN8644-COINCIDENTE. The authors wish to thank J. M. Camas-Albar from Indra Sistemas S.A. for his help. This work has been additionally funded by Xunta de Galicia, Ministerio de Ciencia e Innovacin of Spain, and FEDER funds of the European Union under grants with numbers 2012/287, TEC2010-19545-C04-01, and CSD2008-00010.

References

1. OFDMA PHY SAP Interface Specification for 802.16 Broadband Wireless Access Base Stations. Tech. rep., Intel Corporation (2007).
2. IEEE Standard for Local and metropolitan area networks Part 16: Air Interface for Broadband Wireless Access Systems Amendment 3: Advanced Air Interface. IEEE Std 802.16m-2011(Amendment to IEEE Std 802.16-2009) (2011). doi:10.1109/IEEESTD.2011.5765736.
3. IEEE Standard for Air Interface for Broadband Wireless Access Systems. IEEE Std 802.16-2012 (Revision of IEEE Std 802.16-2009) (pp. 1–2542) (2012).10.1109/IEEESTD.2012.6272299.
4. IEEE Standard for Air Interface for Broadband Wireless Access Systems–Amendment 1: Enhancements to support machine-to-machine applications. IEEE Std 802.16p-2012 (Amendment to IEEE Std 802.16-2012) (pp. 1–82) (2012). doi:10.1109/IEEESTD.2012.6327306.
5. IEEE Standard for WirelessMAN-Advanced Air Interface for Broadband Wireless Access Systems. IEEE Std 802.16.1-2012 (pp. 1–1090) (2012). doi:10.1109/IEEESTD.2012.6297413.
6. IEEE Standard for WirelessMAN-Advanced Air Interface for Broadband Wireless Access Systems Amendment 1: Enhancements to support machine-to-machine applications. IEEE Std 802.16.1b-2012 (Amendment to IEEE Std 802.16.1-2012) (pp. 1–126) (2012). doi:10.1109/IEEESTD.2012.6328224.
7. Ansari, A., Rajput, A., Hashmani, M. (2009). WiMAX network optimization—analyzing effects of adaptive modulation and coding schemes used in conjunction with ARQ and HARQ. In *Seventh annual communication networks and services research conference, 2009. CNSR '09* (pp. 6–13). doi:10.1109/CNSR.2009.12.
8. Carro-Lagoa, A., Suarez-Casal, P., Garcia-Naya, J., Fraga-Lamas, P., Castedo, L., Morales-Mendez, A. (2013). Design and implementation of an OFDMA-TDD physical layer for WiMAX applications. *EURASIP Journal on Wireless Communications and Networking*, *2013*(1), 243. doi:10.1186/1687-1499-2013-243. http://jwcn.eurasipjournals.com/content/2013/1/243.
9. Chuang, G., Ting, P.A., Hsu, J.Y., Lai, J.Y., Lo, S.C., Hsiao, Y.C., Chiueh, T.D. (2011). A MIMO WiMAX SoC in 90nm CMOS for 300km/h mobility. In *IEEE international solid-state circuits conference digest of technical papers (ISSCC), 2011* (pp. 134–136). doi:10.1109/ISSCC.2011.5746252.

10. Colda, R., Palade, T., Pucchita, E., Vermecan, I., Moldovan, A. (2010). Mobile WiMAX: system performance on a vehicular multipath channel. In *Proceedings of the fourth european conference on antennas and propagation (EuCAP), 2010* (pp. 1–5).
11. Cox, R., & Sundberg, C. (1994). An efficient adaptive circular Viterbi algorithm for decoding generalized tailbiting convolutional codes. *IEEE Transactions on Vehicular Technology*, *43*(1), 57–68. doi:10.1109/25.282266.
12. Hempel, M., Wang, W., Sharif, H., Zhou, T., Mahasukhon, P. (2008). Implementation and performance evaluation of Selective Repeat ARQ for WiMAX NS-2 model. In *33rd IEEE conference on local computer networks, 2008. LCN 2008* (pp. 230–235). doi:10.1109/LCN.2008.4664174.
13. Hu, S., Wu, G., Guan, Y.L., Law, C.L., Yan, Y., Li, S. (2007). Development and performance evaluation of mobile WiMAX testbed. In *IEEE mobile WiMAX symposium, 2007* (pp. 104–107). doi:10.1109/WIMAX.2007.348688.
14. Imperatore, P., Salvadori, E., Chlamtac, I. (2007). Path loss measurements at 3.5 GHz: a trial test WiMAX based in rural environment. In *3rd international conference on testbeds and research infrastructure for the development of networks and communities, 2007. TridentCom 2007* (pp. 1–8). doi:10.1109/TRIDENCOM.2007.4444709.
15. Chang, K.-C., Lin, J.-W., Chiueh, T.D. (2007). Design of a downlink baseband receiver for IEEE 802.16E OFDMA mode in high mobility. In *IEEE international SOC conference, 2007* (pp. 301–304).
16. Lai, H., & Boumaiza, S. (2008). WiMAX baseband processor implementation and validation on a FPGA/DSP platform. In *Canadian conference on electrical and computer engineering, 2008. CCECE 2008* (pp. 001,449–001,452). doi:10.1109/CCECE.2008.4564781.
17. Latkoski, P., & Popovski, B. (2009). Delay and throughput analysis of IEEE 802.16 ARQ mechanism. In *International conference on wireless and optical communications networks, 2009. WOCN '09. IFIP* (pp. 1–5). doi:10.1109/WOCN.2009.5010534.
18. Mahmoud, H., Arslan, H., Ozdemir, M. (2006). Initial ranging for WiMAX (802.16e) OFDMA. In *IEEE military communications conference, 2006. MILCOM 2006* (pp. 1–7). doi:10.1109/MILCOM.2006.302240.
19. Mehlführer, C., Caban, S., Rupp, M. (2008). Experimental evaluation of adaptive modulation and coding in MIMO WiMAX with limited feedback. *EURASIP Journal on Advances in Signal Processing*, *2008*. doi:10.1155/2008/837102.
20. Mohamed, M.A., Zaki, F.W., Mosbeh, R.H. (2010). Simulation of WiMAX Physical Layer: IEEE 802.16e. *IJCSNS International Journal of Computer Science and Network Security*, *10*(11).
21. Ohseki, T., Morita, M., Inoue, T. (2007). Burst construction and packet mapping scheme for OFDMA Downlinks in IEEE 802.16 Systems. In *IEEE global telecommunications conference, 2007. GLOBECOM '07* (pp. 4307–4311). doi:10.1109/GLOCOM.2007.819.
22. Pareit, D., Lannoo, B., Moerman, I., Demeester, P. (2012). The history of WiMAX: a complete survey of the evolution in certification and standardization for IEEE 802.16 and WiMAX. *IEEE Communications Surveys Tutorials*, *14*(4), 1183–1211. doi:10.1109/SURV.2011.091511.00129.
23. Pareit, D., Petrov, V., Lannoo, B., Tanghe, E., Joseph, W., Moerman, I., Demeester, P., Martens, L. (2010). A throughput analysis at the MAC Layer of Mobile WiMAX. In *IEEE wireless communications and networking conference (WCNC), 2010* (pp. 1–6). doi:10.1109/WCNC.2010.5506379.
24. Sayenko, A., Tykhomyrov, V., Martikainen, H., Alanen, O. (2007). Performance analysis of the IEEE 802.16 ARQ mechanism. In *Proceedings of the 10th ACM symposium on modeling, analysis, and simulation of wireless and mobile systems, MSWiM '07* (pp. 314–322). New York: ACM. doi:10.1145/1298126.1298180.
25. Schmidl, T., & Cox, D. (1997). Robust frequency and timing synchronization for OFDM. *IEEE Transactions on Communications*, *45*(12), 1613–1621. doi:10.1109/26.650240.
26. So-In, C., Jain, R., Tamimi, A.K. (2009). Scheduling in IEEE 802.16e mobile WiMAX networks: key issues and a survey. *IEEE Journal on Selected Areas in Communications*, *27*(2), 156–171. doi:10.1109/JSAC.2009.090207.
27. Suárez-Casal, P., Carro-Lagoa, A., García-Naya, J., Castedo, L. (2010). A multicore SDR architecture for reconfigurable WiMAX Downlink. In *13th Euromicro conference on digital system design: architectures, methods and tools (DSD), 2010* (pp. 801–804). doi:10.1109/DSD.2010.108.
28. Wu, M., Wu, F., Xie, C. (2008). The design and implementation of WiMAX base station MAC based on Intel Network Processor. In *International conference on embedded software and systems symposia, 2008. ICESS Symposia '08* (pp. 350–354). doi:10.1109/ICESS.Symposia.2008.46.
29. Wu, Y.J., Lin, J.M., Yu, H.Y., Ma, H.P. (2009). A baseband testbed for uplink mobile MIMO WiMAX communications. In *IEEE international symposium on circuits and systems, 2009. ISCAS 2009* (pp. 794–797). doi:10.1109/ISCAS.2009.5117874.
30. Zaggoulos, G., Tran, M., Nix, A. (2008). Mobile WiMAX system performance—simulated versus experimental results. In *IEEE 19th international symposium on personal, indoor and mobile radio communications, 2008. PIMRC 2008* (pp. 1–5). doi:10.1109/PIMRC.2008.4699670.

Pedro Suárez-Casal received a Computer Engineering degree in 2008, and a M. Sc. degree in ICT for Mobile Networks in 2009 from Universidade da Coruña (UDC). Since 2008 he has been working in the Group of Electronic Technology and Communications (GTEC) at the Department of Electronics and Systems at UDC where he is currently pursuing his PhD degree. His main interest fields are signal processing and digital communications with special emphasis on estimation/equalization of MIMO-OFDM channels in high mobility scenarios and real time digital signal processing with DSPs and FPGAs. He is co-author of six papers published in indexed journals and international conferences. He has also been researcher in multiple projects funded by public organisms and private companies.

Ángel Carro-Lagoa received a Computer Engineering degree and a M. Sc. degree in ICT for Mobile Networks from University of A Coruña (UDC), Spain, in 2007 and 2009 respectively. He has been working in the Group of Electronic Technology and Communications (GTEC) at the UDC since 2007. He is co-author of five papers published in indexed journals and international conferences. His main research interests are multicarrier communication systems and real time digital signal processing using DSPs and FPGAs.

José A. García-Naya was born in A Coruña in 1981. He studied Computer Engineering at the University of A Coruña (UDC), Spain, where he obtained his degree "Ingeniero en Informtica" in 2005, and his Ph.D. degree with the distinction "Doctor with European Mention" in 2010. Since 2005 he is with the Group of Electronic Technology and Communications (GTEC) at the UDC, where he is currently Associate Professor. Since 2008 he spent several months at the Institute of Telecommunications at the Vienna University of Technology collaborating in the experimental evaluation of mobile communications systems. José A. is co-author of a patent, more than 15 articles published in peer-reviewed international journals, 4 book chapters and more than 30 contributions to international conferences. He has also been member of the research team in more than 20 research projects funded by public institutions and private companies. His research interests are in the field of digital communications, with special emphasis on the experimental evaluation of wireless communication systems.

Paula Fraga-Lamas received a M. Sc. degree in Computer Engineering and a M. Sc. degree in ICT for Mobile Networks from Universidade da Coruña (UDC) Spain, in 2008 and 2011 respectively. Since 2009 she has been working in the Department of Electronics and Systems at UDC where she is currently pursuing her PhD degree. She is co-author of five papers published in international indexed journals and conferences. Her current research interests include MIMO, LTE and WiMAX systems. Since July 2012 is part of the exploratory team RTO-IST-ET-068 of the IST (Information Systems Technology) panel of NATO STO (Science and Technology Organization) to explore the potential applicability of commercial technologies to the next-generation tactical networks. She has also been participating in several research projects funded by the regional and national government as well as R+D contracts with private companies.

Luis Castedo is a Professor in the School of Computer Engineering at Universidade da Coruña, Spain. He received the Ingeniero de Telecomunicación and Doctor Ingeniero de Telecomunicación degrees, from Universidad Politécnica de Madrid, Spain, in 1990 and 1993, respectively. Since 1994 he has been a faculty member in the Department of Electronics and Systems at UDC and chairman of the Department between 2003 and 2009. Prof. Castedo is coauthor of more than 150 papers in peer-reviewed international journals and conferences, holds one patent and has contributed to three books. He has also been principal researcher in more than 50 research projects funded by public organisms and private companies. His papers have received two best student paper awards at the IEEE/ITG Workshop on Smart Antennas in 2007 and at the 14th IEEE International Workshop on Signal Processing Advances in Wireless Communications in 2013. Prof. Castedo has been actively involved in committees and conference organization. In particular, he has been the General Chair of the 18th National Symposium URSI in 2003 and of the 8th IEEE Sensor Array and Multichannel Signal Processing Workshop in 2014. His research interests are signal processing and digital communications with special emphasis on blind adaptive filtering, estimation/equalization of MIMO channels, space-time coding and prototyping of digital communication equipments.

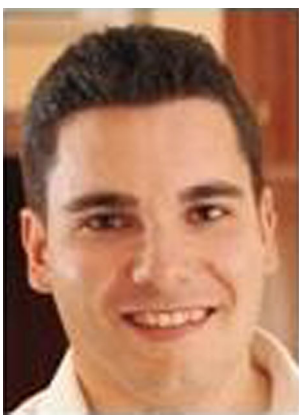

Antonio Morales-Méndez was born in Madrid, Spain, in May 1982. He received the degree in Telecommunications Engineering from Universidad Carlos III in 2007. Final Degree Project was related with multicarrier modulations and MIMO techniques modeling in Matlab/Simulink. He has been working in Indra since 2007 as System Engineer. His main responsibilities in Indra are related to Software Defined Radio technology, multicarrier communications systems, real time digital signal processing using DSPs and FPGAs and System Engineering activities (requirements, software design and tests definition).